SAE Aero Design Technical Report

Northern Arizona University

NAU Micro Class

Team #324

Jacob Cabanyog

Devin duBois

Gabriela Liquidano

Iain Pettit

Alexander Veirhout

Alec Zodrow

Certificate of Compliance

APPENDIX A - STATEMENT OF COMPLIANCE

Certification of Qualification

Team Name	NAU Micro Class	Team Number	324
School	Northern Arizona University		
Faculty Advisor	David Willy		
Faculty Advisor's Email	David.Willy@nau.edu		

Statement of Compliance

As faculty Adviser:

DW
_____ (Initial) I certify that the registered team members are enrolled in collegiate courses.

DW
_____ (Initial) I certify that this team has designed and constructed the radio-controlled aircraft in the past nine (9) months with the intention to use this aircraft in the **2023** SAE Aero Design competition, without direct assistance from professional engineers, R/C model experts, and/or related professionals.

DW
_____ (Initial) I certify that this year's Design Report has original content written by members of this year's team.

DW
_____ (Initial) I certify that all reused content have been properly referenced and is in compliance with the University's plagiarism and reuse policies.

DW
____ (Initial) I certify that the team has used the Aero Design inspection checklist to inspect their aircraft before arrival at Technical Inspection and that the team will present this completed checklist, signed by the Faculty Advisor or Team Captain, to the inspectors before Technical Inspection begins.

3/6/2023

Signature of Faculty Advisor — Date

3/6/2023

Signature of Team Captain — Date

Note: **A copy of this statement needs to be included in your Design Report as page 2 (Reference Section 4.3)**

2D Drawings

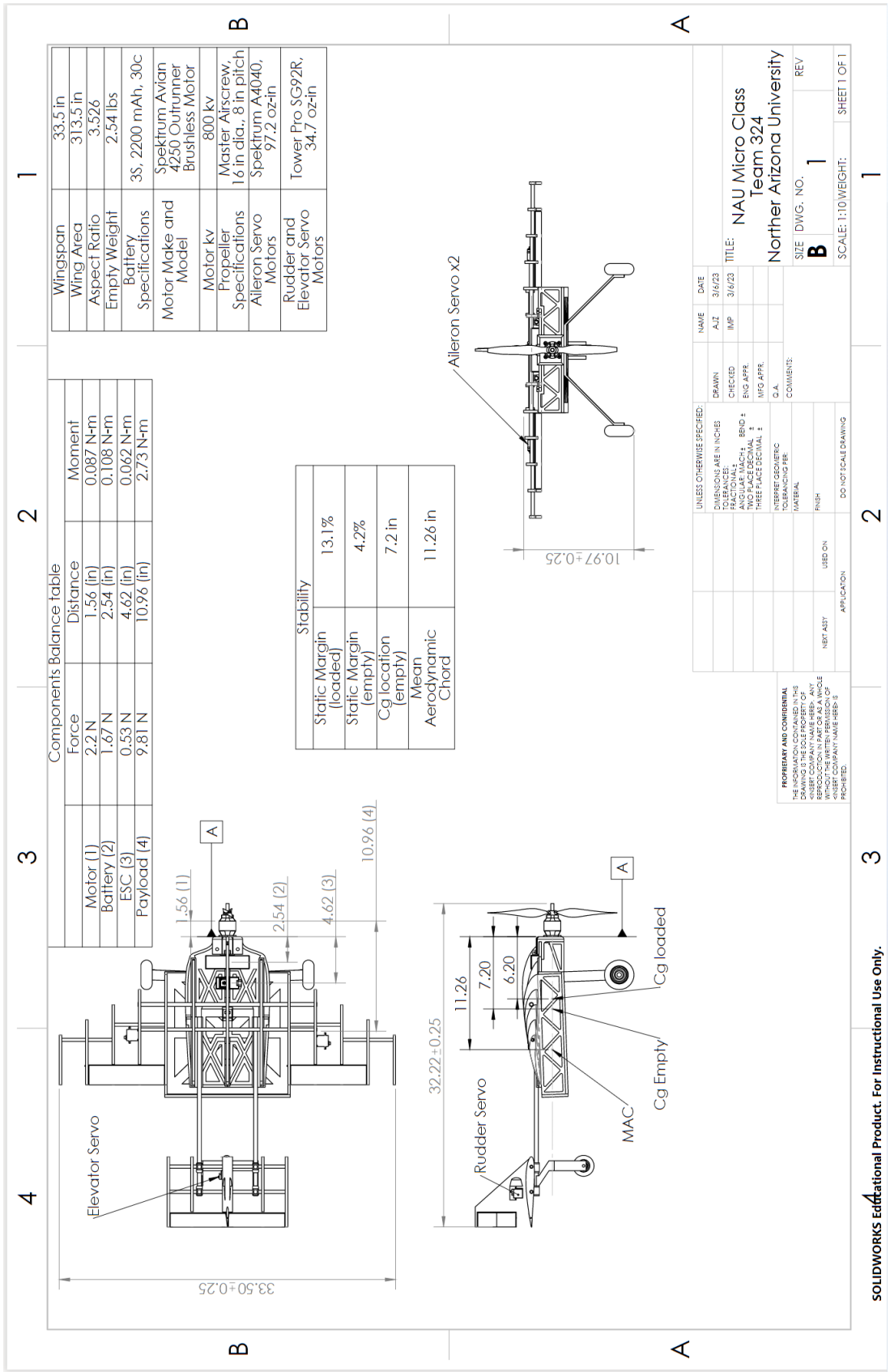
Wingspan 33.5 in
Wing Area 313.5 in
Aspect Ratio 3.526
Empty Weight 2.54 lbs
Battery Specifications 3S, 2200 mAh, 30c
Motor Make and Model Spektrum Avian 4250 Outrunner Brushless Motor
Motor kv 800 kv
Propeller Specifications Master Airscrew, 16 in dia., 8 in pitch
Aileron Servo Motors Spektrum A4040, 97.2 oz-in
Rudder and Elevator Servo Motors Tower Pro SG92R, 34.7 oz-in
Components Balance table
Force Distance Moment
Motor (1) 2.2 N 1.56 (in) 0.087 N-m
Battery (2) 1.67 N 2.54 (in) 0.108 N-m
ESC (3) 0.53 N 4.62 (in) 0.062 N-m
Payload (4) 9.81 N 10.96 (in) 2.73 N-m
Stability
Static Margin (loaded) 13.1%
Static Margin (empty) 4.2%
Cg location (empty) 7.2 in
Mean Aerodynamic Chord 11.26 in
Aileron Servo x2
10.97±0.25
Elevator Servo
33.50±0.25
1.56 (1)
2.54 (2)
4.62 (3)
10.96 (4)
Rudder Servo
32.22±0.25
11.26
7.20
6.20
MAC
Cg Empty
Cg loaded
PROPRIETARY AND CONFIDENTIAL
THE INFORMATION CONTAINED IN THIS DRAWING IS THE SOLE PROPERTY OF <INSERT COMPANY NAME HERE>. ANY REPRODUCTION IN PART OR AS A WHOLE WITHOUT THE WRITTEN PERMISSION OF <INSERT COMPANY NAME HERE> IS PROHIBITED.
UNLESS OTHERWISE SPECIFIED:
DIMENSIONS ARE IN INCHES
TOLERANCES:
FRACTIONAL ±
ANGULAR: MACH ± BEND ±
TWO PLACE DECIMAL ±
THREE PLACE DECIMAL ±
INTERPRET GEOMETRIC TOLERANCING PER:
MATERIAL
FINISH
DO NOT SCALE DRAWING
NAME DATE
DRAWN AJZ 3/6/23
CHECKED IMP 3/6/23
ENG APPR.
MFG APPR.
Q.A.
COMMENTS:
NEXT ASSY
USED ON
APPLICATION
TITLE: NAU Micro Class Team 324 Norther Arizona University
SIZE B
DWG. NO. 1
REV
SCALE: 1:10 WEIGHT:
SHEET 1 OF 1
SOLIDWORKS Educational Product. For Instructional Use Only.

Technical Data Sheet: Aircraft Performance Prediction

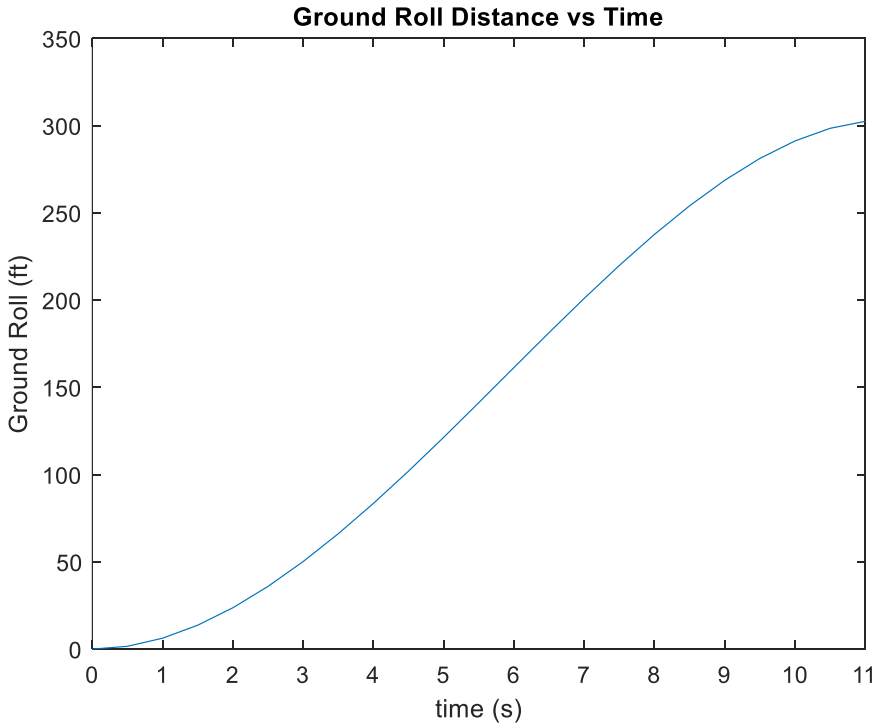

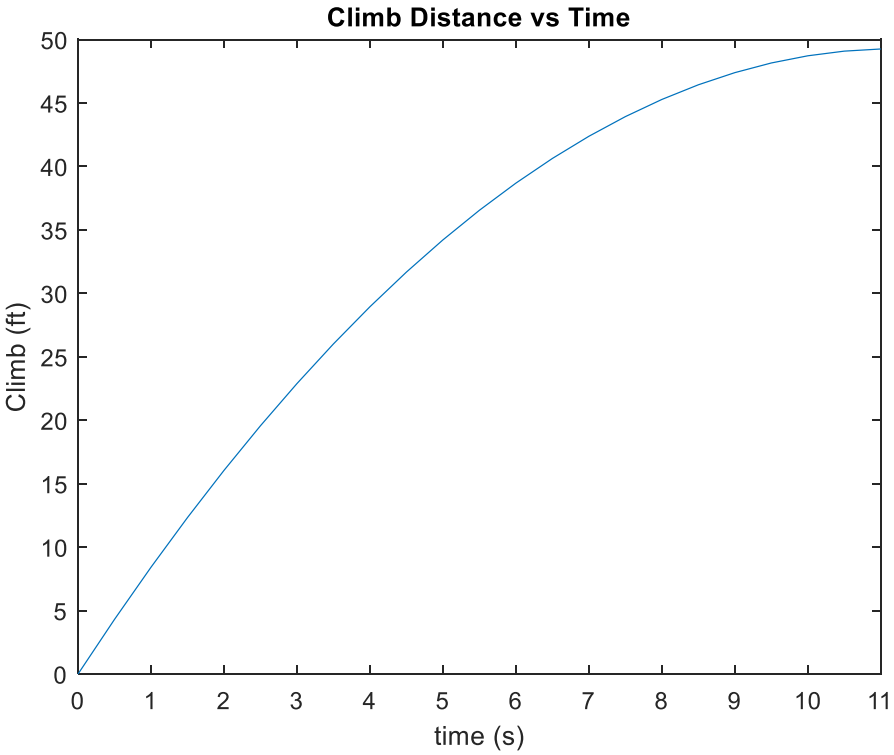

Table of Contents

Table of References

[1] “Aileron design Chapter 12 design of Control Surfaces - aero.us.es.” [Online]. Available: http://aero.us.es/adesign/Slides/Extra/Stability/Design_Control_Surface/Chapter%2012.%20Desig%20of%20Control%20Surfaces%20(Aileron).pdf. [Accessed: 05-Feb-2023].

[2] “Balancing RC airplanes - how to,” *RC Airplane World - Complete Beginners RC Flying Guide*. [Online]. Available: https://www.rc-airplane-world.com/balancing-rc-airplanes.html#:~:text=Methods%20of%20Balancing%20RC%20Airplanes%201%20Ballasting%20Up,plane.%20...%203%20Roll%20Balancing%20RC%20Airplanes%20. [Accessed: 05-Feb-2023].

[3] M. Bedding, “Control surface flutter, balance, and Vne,” *Motion RC*, 13-Oct-2020. [Online]. Available: https://www.motionrc.com/blogs/motion-rc-blog/control-surface-flutter-balance-and-vne. [Accessed: 05-Feb-2023].

[4] “Primary flight control surfaces and dual purpose flight control surfaces of a fixed-wing aircraft,” *Aircraft Systems*. [Online]. Available: https://www.aircraftsystemstech.com/p/flight-control-surfaces-directional.html. [Accessed: 05-Feb-2023].

[5] W. F. Durand, Aerodynamic theory. Internet Archive, 1934.

[6] Tyto Robotics, “Series 1580-1585,” Tyto Robotics. [Online]. Available: https://www.tytorobotics.com/pages/series-1580-1585. [Accessed: 11-Nov-2022].

[7] Brezina and S. Thomas, “Measurement of static and dynamic performance characteristics of Electric Propulsion Systems,” 51st AIAA Aerospace Sciences Meeting including the New Horizons Forum and Aerospace Exposition, May 2013.

[8] M. Khasyofi and F. Hartono, “Development testing method and analysis static thrust for propeller based propulsion,” IOP Conference Series: Materials Science and Engineering, vol. 645, no. 1, p. 012015, 2019.

[9] *Racerstar Brushless Motor Thrust stand v3 for 11mm-59mm outrunner motor*. [Online]. Available: https://www.racerstar.com/racerstar-brushless-motor-thrust-stand-v3-for-11mm-59mm-outrunner-motor-p-199.html. [Accessed: 09-Dec-2022].

[10] A. Depperois, “About Stability Analysis using XFLR5.” Nov-2010

[11] “Computational Fluid Dynamics,” *Computational Fluid Dynamics - an overview | ScienceDirect Topics*. [Online]. Available: https://www.sciencedirect.com/topics/materials-science/computational-fluid-dynamics#:~:text=Computational%20fluid%20dynamics%20(CFD)%20is,and%20energy)%20governing%20fluid%20motion. [Accessed: 05-Feb-2023].

[12] J. D. Anderson, *Aircraft Performance and Design*. Boston, MA: McGraw-Hill Higher education, 2012.

Table of Figures

Table of Tables

Table of Nomenclature

Re	Reynold's Number
ν	Kinematic Viscosity
$V \& V_T$	Velocity of Aircraft
c_{avg}	Average Characteristic Length
F_L	Force of Lift
C_L	Coefficient of Lift
C_D	Coefficient of Drag
ρ	Air Density
A_p	Wing Planform Area
$V_{takeoff}$	Instantaneous Velocity at Takeoff
F_∞	Applied Pressure of Working Fluid
A_{wetted}	Wetted Surface Area
θ	Angle of Deflection
F_T	Torque
L_{arm}	Servo Lever Arm
L_A	Rolling Moment
S	Reference Area
$\overline{q}$	Dynamic Pressure
C_l	Rolling Moment Coefficient
b	Wingspan
TV	Tail Volume Coefficient
LA_{elev}	Moment Arm of Elevator
$Area_{elev}$	Area of Elevator
MAC_{wing}	Mean Aerodynamic Cord
$Area_{wing}$	Area of Wing
X_{NP}	Position Neutral Point
X_{CG}	Position Center of Gravity
P	Power
A	Current
V	Voltage
C_T	Coefficient of Thrust
T	Thrust
n	Angular Velocity
D	Propellor Diameter
C_p	Coefficient of Power
P_p	Propellor Power

Executive Summary

This technical design report outlines the design and manufacturing process of Northern Arizona University's 2023 SAE Aero Design Team. This team is competing in the Micro Aero class, which is a design competition that entails designing and manufacturing a brushless motor driven remote controlled (RC) aircraft capable of carrying cargo. The team will be scored on their design's payload capacity as well as their flight speed. Per competition requirements, the aircraft will be limited to a takeoff distance of 8 feet and will have to fly an additional 300 feet before making a 180-degree turn. The team must then fly at least another 300 feet before making a second 180-degree turn. The aircraft must land within 200 feet of the designated landing area. The aircraft is limited to a battery that supplies no more than 450 Watts of power to the propulsion system and must have a wingspan that does not exceed 36 inches. This year's team will focus on reducing empty weight of the plane to increase acceleration and weighted payload capacity of the plane. The finalized design will be carrying a single 12"x12"x2" payload box to maximize the final flight score at competition. This report will outline the thought process of the team throughout the project and explain how the team was able to optimize aircraft weight, thrust, lift, and drag.

Team Strategy

Selection of Aircraft Configuration

Critical Performance Factors

To begin the process of designing aircraft features such as the wings, the team first determined critical performance factors that will be the team's working conditions when in flight. Determining the critical Reynolds Numbers, the Reynolds Numbers at takeoff and at max cruising speed, was the design teams first step. This Reynolds Numbers for the wings were calculated using **Equation 1** shown below.

$$Re = \frac{V * c_{avg}}{\nu} \quad (1)$$

Using the anticipated velocity at takeoff and the kinematic viscosity in Fort Worth, Texas air conditions, the team found the takeoff Reynolds number to be approximately 17,000. Substituting our anticipated cruising velocity of 40 ft/s, the Reynolds number was found to be approximately 193,000. Now knowing these critical parameters, the team was able to compare different airfoil geometries to determine an expected coefficient of lift.

Airfoil Selection

To select the airfoil geometry needed to generate enough lift to takeoff with the competition takeoff parameters, the team analyzed a series of different airfoils using an online airfoil plotter that allowed a comparison of different geometry performances at our critical Reynolds Numbers. The Selig S-1223 airfoil was chosen by the team for its high coefficient in comparison to other airfoils. Plots comparing both the C_L and the C_D for the S-1223 airfoil are shown in **Figure 1** and **Figure 2** below.

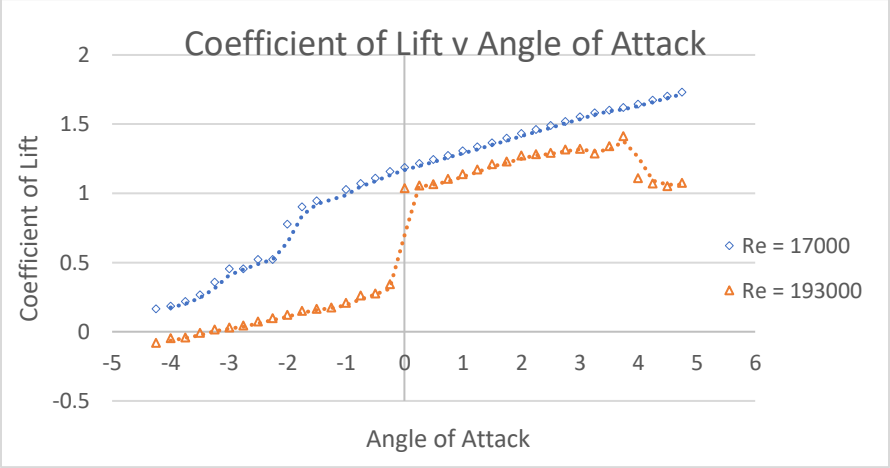

Figure 1: Coefficient of Lift vs Angle of Attack

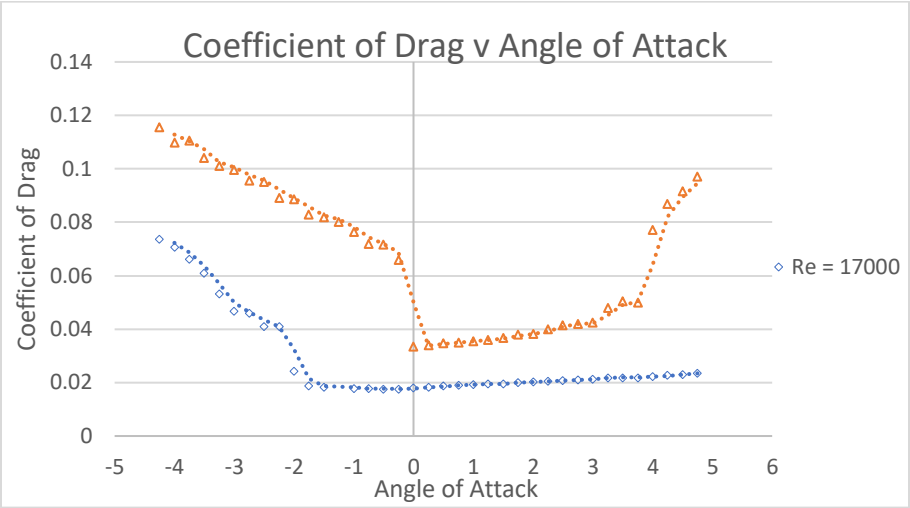

Figure 2: Coefficient of Drag vs Angle of Attack

With a maximum coefficient of lift of 2.2919, the team concluded that this airfoil would provide the most flexibility with general wing geometry, considering the limitations to wingspan per competition constraints.

Wing Geometry

To allow for larger fuselage volume cargo capacity, the team wanted to design around a large wing chord length, to allow space for the 12”x12”x2” cargo box to fit below the wings. The aircraft wing geometry features a tapped leading edge towards the tips of the wing to reduce induced drag on the wing as well as reducing the empty weight of the aircraft. The chord length is taped from its maximum of 14” down to a 5” chord length: an average chord length of 9.5”.

To ensure that these dimensions will provide enough lift at takeoff, the team calculated the 2-D approximation of lift generated by the wings using **Equation 2** below:

$$F_L = C_L * \rho * A_p * \frac{V_{takeoff}{}^2}{2} \quad (2)$$

An approximate lifting force on the plane at takeoff was calculated to be 3.06 lbs.

Static/Dynamic Thrust

The Avian 4250-800Kv Outrunner Brushless Motor was selected for the single-prop design Which is rated for a maximum continuous current of 925 Watts. The aircraft utilizes the required power limiter to bring this continuous wattage down to the competition limit of 450 Watts. To understand the performance of our propulsion system, a static thrust comparison was performed to compare, and contrast thrust outputs of this motor combined with different sized propellers.

The team performed a series of tests to measure the static thrust on three separate propellers. To further optimize the teams current design, this experiment compared the performance of three different propellers. The experiment was performed using a dynamometer and a tachometer. The dynamometer provided the team with the thrust force generated by the propellers spun by the team's brushless motor. The dynamometer was also used to measure the voltage and amperage of the motor to provide the team with means to calculate power draw. The tachometer was used to measure the rotational speed of the motor by placing reflective tape of the spinning shaft of the motor. This enabled the team to create correlations between the rotational speed of the blades and their thrust generation and power consumption.

The measurements taken from the dynamometer are taken to find the power in Watts for each propeller, as well as compare the thrust to each propeller. The tachometer is used to measure the rpms to be plotted against the thrust and power. The measurements are also used to calculate the coefficient of thrust and power to see which propeller has the best coefficients.

To solve for the power [W], **Equation 3** is used, which is the current [A] multiplied by the voltage [V].

$$P = A \cdot V \tag{3}$$

To solve for the Coefficient of thrust, **Equation 4** is used, shown below.

$$C_T = \frac{T}{\rho n^2 D^4} \quad (4)$$

To solve for the Coefficient of power, **Equation 5** is used, shown below.

$$C_p = \frac{P_p}{\rho n^2 D^5} \quad (5)$$

These equations will allow the team to solve for the power and coefficients of thrust and power of each propeller. Using these values to plot against the other propellers to see which type of propeller will be most beneficial to use.

Measuring at around the same rpms for each propeller at 5 different rpms, increasing after each measurement. The first measurement was around 1750 rpms and had 4 more measurements that went up to around 7500 rpms. The first test was the 13” diameter propeller and ran the test twice to get accurate data. Then repeating the process with the 12” diameter propeller, and then the 8” diameter propeller.

Using the dynamometer to collect the data, the team plotted thrust generation against motor rotational speed ranging from 2000 rpm up to 7840 rpm. The relationship between thrust and rpm is displayed in **Figure 3** below.

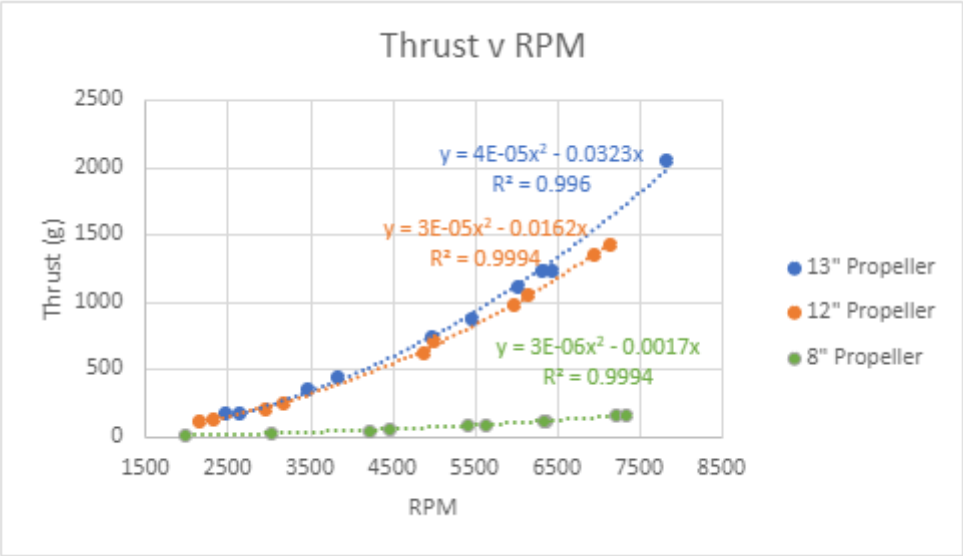

Figure 3: Thrust v RPM

The team concluded that as the rotational speed of the motor was increased, the thrust generated by the propeller grew exponentially for all three propellers. The 13” propeller generated the largest thrust forces in comparison to the smaller diameter propellers. The 13” propeller generated a maximum thrust force of 2050 grams at a rotational speed of 7840 rpm. The thrust generated by this propeller was 13.22 times greater that the thrust generated at the same rotational speed by the 8” propeller, confirming that a larger diameter propeller does generate more lift. To ensure that our plane will generate enough lift considering this limitation, thrust generation was compared against power consumption in **Figure 4**.

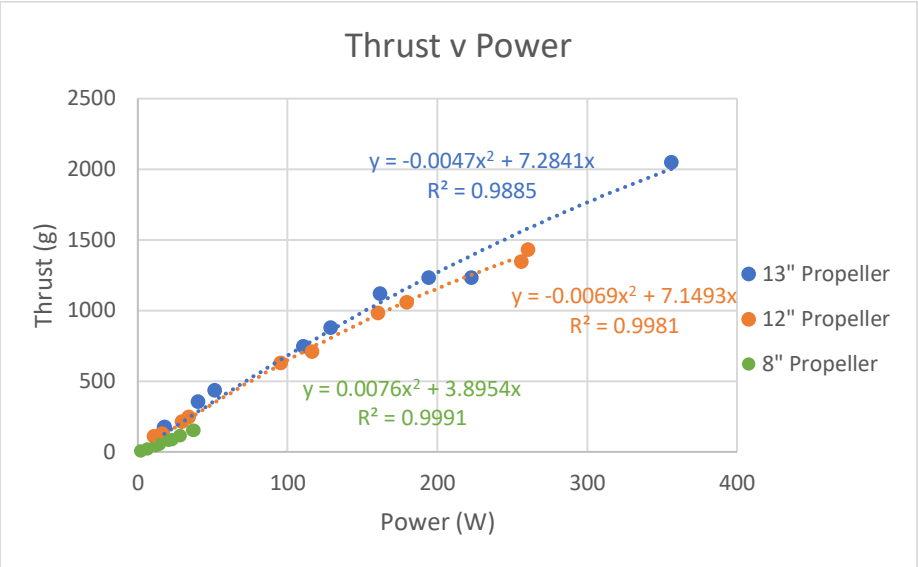

Figure 4: Thrust v Power

The relationship shows that once again, the 13” propeller outperformed the smaller propellers. As displayed in **Figure 4**, the 8” propeller and the 12” propeller were unable to reach the same maximum power consumption as the 13” propeller. This is because it takes less energy to spin a smaller propeller at the same rotational speed than a larger propeller. Since the motor has a maximum rotation rate, the same power draw was not achievable for all three configurations. At 356.4 W of power consumption, the 13” propeller was able to generate 2050 gram of thrust. However, there is a tradeoff to take note of. As the rotational speed is increased, the power consumption also increases exponentially, as demonstrated with **Figure 5** below.

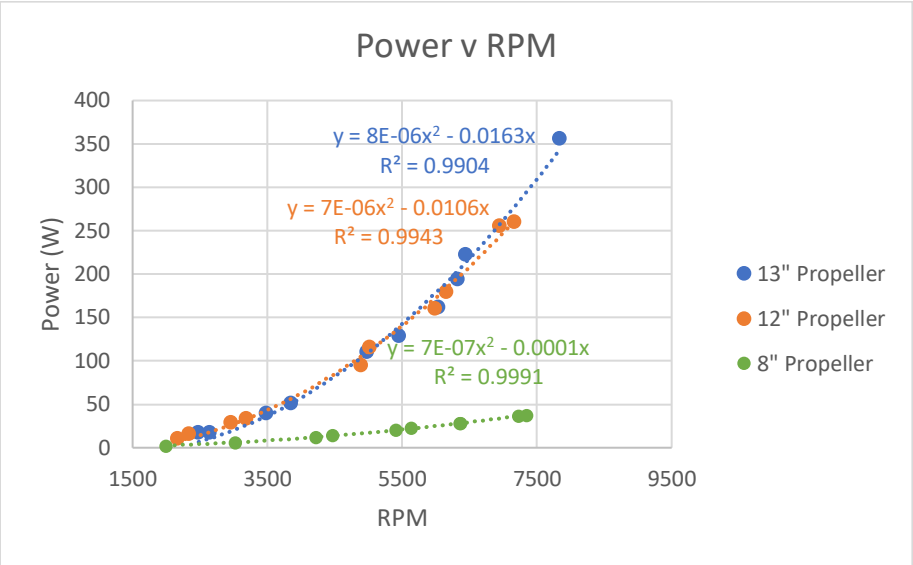

Figure 5: Power v RPM

The 8” propeller had the best performance when comparing power against rotational speed. At a rotational speed of 7344 rpm, the power consumption was only 37.60 W. For comparison, at the same rotational speed, the 13” propeller would be consuming 311.77 W.

Using both **Equation 4** and **Equation 5**, the team found these coefficients to remove the effects of air density, rotational speed, and propeller diameter. This allowed the team to analyze the true performance of each propeller, negating the effects of the mentioned variables. The average of the ten trials for each propeller was found and compiled into **Table 1**.

Table 1: Coefficients of Thrust and Power

Propeller	Average Coefficient of Thrust (C_T)	Average Coefficient of Power (C_P)
8” Propeller	0.0456	0.0722
12” Propeller	0.0853	0.0607
13” Propeller	0.0703	0.0385

Surprisingly, the 12” propeller had the highest coefficient of thrust at an average value of 0.0853. The 8” propeller had a much smaller average value of 0.0456. This leads the team to the conclusion that without the effects of propeller diameter and rotational speed, the 12” propeller was the most effective at generating thrust. With reducing power consumption being a design goal for the team, the 13” propeller would meet that goal the best with a coefficient of power of 0.0385.

The selected airfoil was the 13” diameter propeller for its high thrust generation as well as its low coefficient of power. Our static thrust test produced an expected maximum thrust output from our propulsion system of 4.519 lbs.

Aircraft Empty Weight

After generating an approximate lifting force of 3.06 lbs, the initial maximum weight for the plane was set to three pounds. This weight would allow for the plane to fly given the lifting force was greater than three pounds. After the conclusion of the thrust analysis, a more accurate weight goal could be set to optimize the planes thrust to weight ratio. The optimal thrust weight ratio selected was two. Given a thrust of 4.519 lbs, the final empty weight goal of the plane was 2.25 lbs. As parts were manufactured, they were weighed and inserted into our SOLIDWORKS using a mass override feature. This ensured that our total plane weight accurate and gave the team an accurate position of our center of mass to assist in a stability analysis within XFLR5.

Aircraft Stability and Control

Control for a fixed-wing aircraft takes place around the lateral, longitudinal, and vertical axes. The ailerons, which are attached to the trailing edge of both wings move the aircraft about the longitudinal axis causing it to roll. The elevators, on the other hand, are attached to the trailing edge of the horizontal stabilizer and when moved, it alters the aircrafts pitch. This causes the plane to move about the lateral axis. Lastly, the rudder is hinged to the trailing edge of the vertical stabilizer and when its position is

changed, the plane rotates about the vertical axis. It is critical for the primary flight control surfaces to be balanced so they do not vibrate or flutter in the wind. [4]

The team found that an aircraft's successful performance heavily relies on its maneuverability. This implies thrust, aircraft mass moment of inertia and control power. Since the ailerons cause the aircraft to steer along its three-dimensional flight path to a specified destination, the team found that an aileron's main goal is roll control. To properly design an aileron, the team must determine four parameters. These parameters include the aileron area, chord/span, maximum and minimum deflection, and the location of the inner edge of the aileron along the wingspan. Based on extensive research, the group found that 5 to 10 percent of the wingspan is devoted to the aileron. 15 to 25 percent is the aileron to wing chord ratio and 20-30 percent is the aileron to wingspan ratio. Lastly, 60 to 80 percent is the inboard aileron span. Given these statistics, the team's CAD model seems to correlate respectively with each percentage. [1]

Another critical note the team must take into consideration is the aircraft's balance and flutter. Flutter is essentially instability due to the aircraft's interaction with aeroelasticity. Balancing the control surfaces will help reduce the effects of flutter. By balancing the aircraft correctly, this will also reduce the load on the servo gear. By calculating the forces applied on the control surfaces, the team may be able to navigate any potential flutter before competition. This will allow the team to ensure their servos are properly sized or if they need to purchase a different size. [3]

Control Surfaces Analysis

To be able to estimate the forces applied on each control surface, some assumptions about the conditions of the aircraft were made. The first assumption is that at the leading edge of each control surface, the air is flowing parallel to the surface. This implies that when the control surfaces are not angled away from

their cruising position, there is no pressure applied from the working fluid. This also implies that the largest resulting force from the fluid will occur when the control surfaces are deflected at their maximum angle from their resting position. The team also assumed standard sea level air conditions to accurately represent flying conditions in Fort Worth, Texas which has an average elevation of 500 feet.

The rudder and elevator are located on the tail portion of the plane. The elevator is a long strip that spans the backend of the horizontal stabilizer. The elevator has a chord length of 1.4 inches and a span of 11.4 inches. The rudder is located along the trailing edge of the vertical stabilizer. The rudder has a chord length of 1.4 inches, with a span of 3.77 inches.

The first step in analyzing the effectiveness of our control surfaces was calculating the force that would be applied by the air. To do this, this team first identified our load case by defining our maximum speed as 12.192 m/s. The max stress on the control surfaces would occur at this load case speed and would also occur at our maximum angle of deflection from each surface's resting point. The maximum angle that our surfaces would be deflected to is 30 degrees. With our load case defined, **Equation 6** was used to calculate the applied pressure of the working fluid.

$$F_{\infty} = \frac{1}{2} * \rho * V^2 * A_{wetted} * \sin(\theta) \quad (6)$$

The wetted area of each control surface was found using the surface area measuring tool within SolidWorks. The next step to validate our control surface design is to calculate the amount of torque on the servo motors. These torque values for the aileron, rudder, and elevator servos are found using **Equation 7** below:

$$F_T = F_{\infty} * L_{arm} \quad (7)$$

The servo arm lengths were found using the length measurement tool within SolidWorks. This length is defined as the length from the servo motor to the resultant force of the fluid on the control surface. Once these values are found, they can be compared to the industry rated maximum torque values that our servo motors can handle. If our current servo motors are incapable of performing, an adequate servo must be found that can deflect our control surfaces to the desired 30 degrees.

When analyzing the effectiveness of the aircraft's ailerons, the team had to assess its rolling moment. This is the force that causes the plane to roll about its longitudinal axis. This is critical information as the rolling motion increases the angle of attack from the lowering wing whilst decreasing the angle of attack for the rising wing. The rolling moment can be characterized using **Equation 8** below:

$$L_A = \bar{q} S C_l b \tag{8}$$

$\bar{q}$ is the dynamic pressure which is the pressure exerted perpendicular to the direction of the flow. The team found that the dynamic pressure came out to 91.04 pascals which was found using **Equation 9** below:

$$\bar{q} = \frac{1}{2} \rho V_T^2 \tag{9}$$

Where rho is the air density and V is the aircraft's airspeed which was calculated at 12.192 m/s. S in **Equation 5** signifies the wing area, b signifies the wingspan, and C_l is the rolling moment coefficient. As a result, the team found that the rolling moment around the longitudinal axis is about 0.39 N*m.

Using a MATLAB code, the force applied on each control surface was calculated. The resulting force from the working fluid on each aileron was calculated to be 0.4643 N. With an arm length of 0.2567 m, the torque applied to the servo motor is 0.1192 Nm per aileron. This servo will be experiencing double that amount of torque due to our current configuration, which has one centrally located servo motor control

both ailerons in series. The applied force on our elevator was found to be 0.4913 N, giving us a torque of 0.0699 Nm. The applied force of the fluid on the rudder was calculated to be 0.1639 N. With a servo arm of only 0.0711 m, the torque acting on this servo motor is 0.0117 Nm. The servo motors that will be utilized for the plane's elevator and rudder are rated at 0.1412 Nm, and the servo motors utilized for our ailerons are rated above 0.2384 Nm. Therefore, these servo motors will provide enough torque to deflect our control surfaces to the maximum deflection angle.

XFLR5 Analysis

The use of the computational flow dynamics (CFD) software XFLR5 will ensure that the plane is statically stable during its max cruise speed, while also producing positive lift. The positioning and sizing of the tail relative to the main wing is critical for stability during flight. The horizontal tail controls the pitch axis of the plane, and the moment arm it generates depends on how big its planform area is and how far it is from the center of gravity. This can be quantified by the Tail Volume coefficient.

This analysis utilizes CFD software that is based on the Navier Stokes Equations. These are a set of partial differential equations that describe the flow of a fluid. The software meshes a 3-D model of the plane and computes the state of the fluid flow at each section using numerical methods. To do this it must first linearize the Navier Stokes Equations and then solve them using LU Decomposition. The use of numerical methods means that the software can only output approximations and never exact answers. This is acceptable as the approximations are very accurate and are only off on a very small scale.

One major assumption made during the CFD analysis was inviscid flow. This assumption was made because only pitch moments and lift/weight forces are being considered. The shear forces generated from viscous flow are negligible to pitching moments because the direction of the force causes drag and yaw moments.

To conduct a flow simulation, specific airfoils had to first be imported to model the wing and tail configuration. Each airfoil needed to be analyzed over a range of Reynolds Numbers to generate plots for each one, so the software knows how they react to flow. The main wing uses a S1223 foil, and the elevator uses a NACA 2412 foil. The plane can then be modelled using XFLR5. The body of the plane was not included in this model because the software makes a note to not include it. The resulting model can be seen in **Figure 6**.

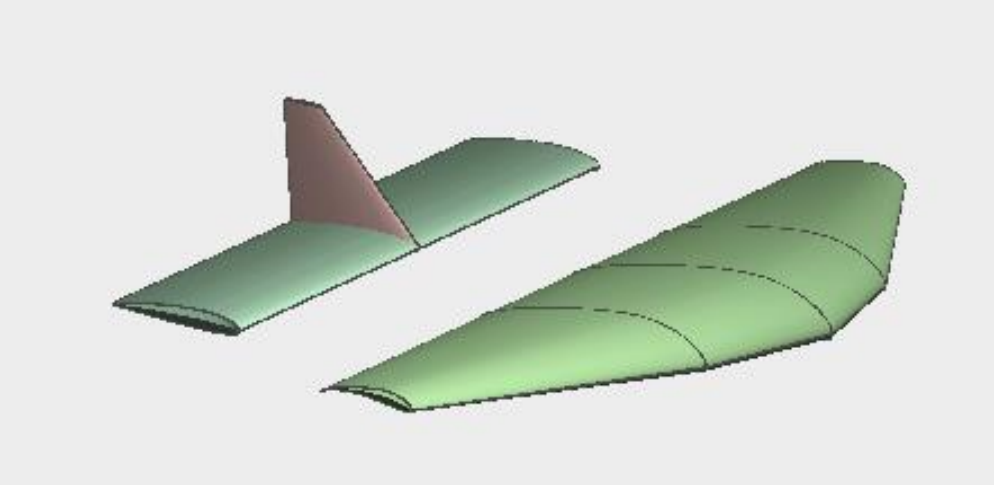

Figure 6: Plane Model

The loading scenario analyzed is at the max cruise speed, which has been assumed to be 12.2 m/s. To get initial approximations of the dimensions, the tail volume was utilized which is a measure of the elevator's capacity to balance the wing's self-pitching moment. The tail volume allowed us to find an appropriate lever arm. To begin an initial tail volume coefficient was assumed to be 0.7. This was pulled from *Aircraft Performance and Design* by John D. Anderson [12]. A MATLAB code was utilized to turn this coefficient into dimensions for the elevator and the placement of it. This was done using **Equation 10** [10].

$$TV = \frac{LA_{elev} * Area_{elev}}{MAC_{Wing} * Area_{Wing}} \quad (10)$$

The dimensions came out to 7 inches in chord length and 12 inches in width, with a 16” distance between the quarter chord points of the wing and tail. The neutral point of an aircraft is the point along its axis where the pitching moment coefficient is not dependent on angle of attack. This sets the rear limit for the center of gravity [10]. This can be found through XFLR5, by iterating different center of gravity locations until the resulting moment coefficient vs. angle of attack graph has a slope of 0. Once this is determined, more iterations need to be conducted until the center of gravity is placed in a manner that the moment coefficient vs. angle of attack graph has a negative slope. By having a negative slope, it shows the plane is in stable static equilibrium, meaning that the pitching moment is balanced, and the plane can fly steadily [10]. The size and positioning of the tail are also iterated to allow for the center of gravity to be in an easily designable position.

The CFD analysis allowed us to iterate the wing and tail configuration to achieve an angle of attack that produces zero pitch moment and generates lift. This was accomplished by running several simulations and analyzing the plots generated. For each iteration, we first analyzed the pitch moment coefficient vs the angle of attack. **Figure 7** shows that when the pitch moment is equal to zero (balanced flight) the angle of attack is approximately 0.5 degrees. **Figure 9** suggests that the plane generates lift at this angle of attack and therefore flies. **Figure 8** further validates this claim by displaying a positive coefficient of lift at the zero-pitch moment position. The center of gravity and neutral point are position 0.183 meters and 0.195 meters away from the nose respectively. The mean aerodynamic chord length is 0.286 meters. The tail chord length is 0.178 meters. The tail width is 0.305 meters. The moment arm is 0.64 meters. The tail volume coefficient is 0.889. These dimensions were used to achieve the graphs depicted in **Figures 7-9** and are listed in **Table 2**.

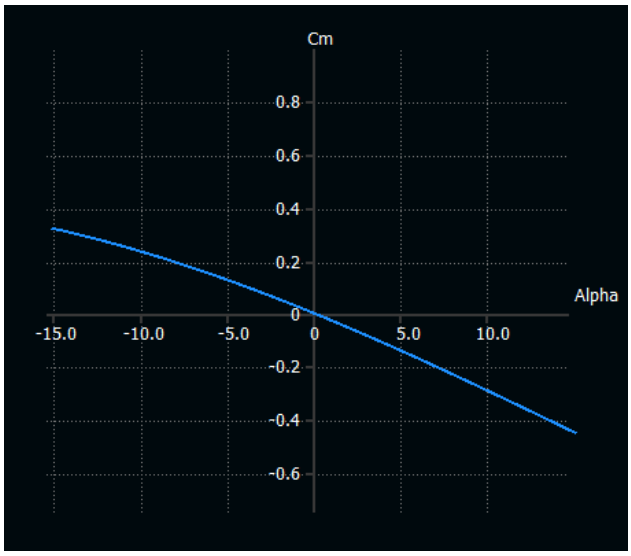

Figure 7: Angle of Attack vs Pitch Moment Coefficient

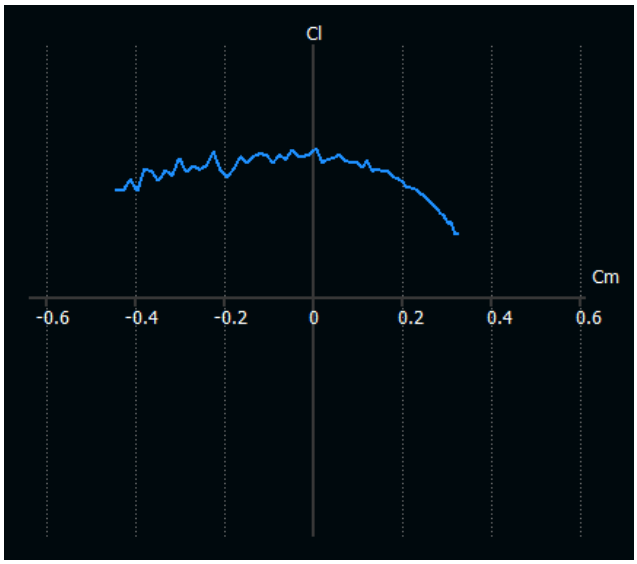

Figure 8: Pitch Moment Coefficient vs Coefficient of Lift

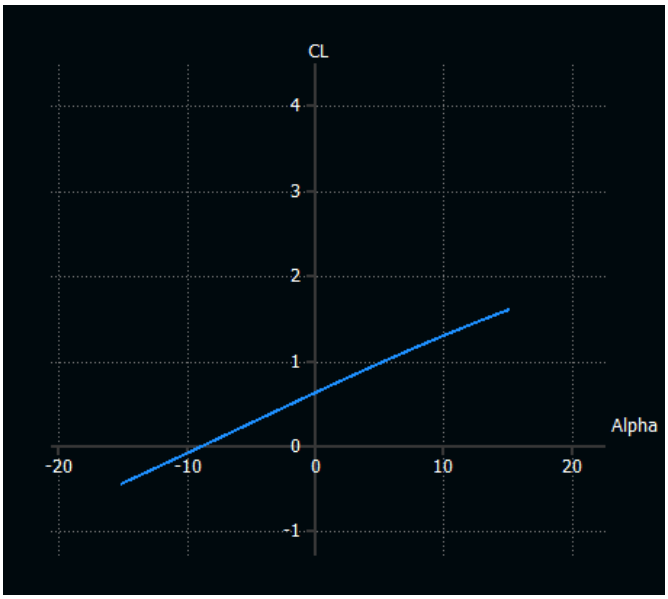

Figure 9: Angle of Attack vs Coefficient of Lift

Table 2: Plane Specifications

Center of Gravity (m)	Neutral Point (m)	Mean Aerodynamic Chord (m)	Tail Chord Length (m)	Tail Width (m)	Tail Moment Arm (m)	Tail Volume Coefficient
0.183	0.195	0.286	0.178	0.305	0.640	0.889

A common margin to measure the moment arms of the plane is through static margin. This is a ratio between the distance between the neutral point and center of gravity and the mean aerodynamic chord of the main wing. This is shown in **Equation 11** below [10].

$$Static\ Margin = \frac{X_{NP} - X_{CG}}{MAC_{wing}} \tag{11}$$

The static margin came out to 4.2% in the empty case. This is relatively low compared to numbers used in *Aircraft Performance and* Design by John D. Anderson [11]. The book referenced that it normally is about 10%. This is not ideal, but it is functionable. The center of gravity was pushed as far forward as possible with the geometry of the model, so some mass engineering is needed to move it forward. For the

loaded case the static margin ended up being 13.1% with a center of gravity 6.2 inches away from the nose. This provides a much more stable flight and is ideal for flight conditions. The analysis was able to determine the sizing and placement of the tail as well as the static margin of the aircraft. The elevator was found to need a chord length of 7 inches and a width of 11.8 inches. It also has a moment arm of 25 inches. The center of gravity must be designed to be 7.2 inches away from the nose of the plane.

Manufacturing

To reduce cost and increase ease of assembly, the final aircraft is designed in a way to be mostly 3D-printed. Using Polylactic Acid (PLA), the team was able to quickly modify and manufacture parts when needed. Going with this path of manufacturing allowed the team to utilize our engineering knowledge to maximize geometry strength rather than relying on material strength. Having 3-dimensional control over part geometry allowed the team to ensure proper fittings and sizing of all parts, while keeping the empty aircraft weight around our final target weight. With control over infill densities of each part, the team was able to add part strength and shift the center of mass when needed. While most of the plane was able to be printed, the plane required multiple high strength support beams. Carbon Fiber tubes with varying thicknesses were utilized to support the wings as well as the tail because carbon fiber has the highest strength-to-weight ratio out of all the materials available to the team. They are also machine very accurately, which ensured that all of their fittings were aligned correctly. Not shown in the 2D drawings, is an aerodynamic shrink wrap, called that will cover all the surfaces of the plane. This will allow the team to reduce the final weight of the plane, as this is a very thin layer of plastic.

Conclusion

Through the process of optimizing their aircraft's weight, thrust, lift, and drag, Northern Arizona University's 2023 SAE Aero Design Team have designed and manufactured a competition ready aircraft. By analyzing the different systems and load cases of the plane, the team was able to analytically

determine exactly how the plane will perform during competition. The team believes in the feasibility of their design and hopes the efforts will translate into success.